

Spring 5-2014

Outlining the Biocidal Mechanisms of Synthetic Antimicrobial Peptide Mimics

Tyler D. Brown
University of Southern Mississippi

Follow this and additional works at: https://aquila.usm.edu/honors_theses

 Part of the [Polymer Science Commons](#)

Recommended Citation

Brown, Tyler D., "Outlining the Biocidal Mechanisms of Synthetic Antimicrobial Peptide Mimics" (2014).
Honors Theses. 252.
https://aquila.usm.edu/honors_theses/252

This Honors College Thesis is brought to you for free and open access by the Honors College at The Aquila Digital Community. It has been accepted for inclusion in Honors Theses by an authorized administrator of The Aquila Digital Community. For more information, please contact Joshua.Cromwell@usm.edu.

The University of Southern Mississippi

Outlining the Biocidal Mechanisms of Synthetic Antimicrobial Peptide Mimics

by

Tyler Dwight Brown

A Thesis
Submitted to the Honors College of
The University of Southern Mississippi
in Partial Fulfillment
of the Requirements for the Degree of
Bachelor of Science
in the Department of Polymer Science

May 2014

Approved by

Sarah E. Morgan, Ph.D., Thesis Adviser
Associate Professor of Polymer Science

Jeffrey S. Wiggins, Ph.D. Chair
Department of Polymer Science

David R. Davies, Ph.D., Dean
Honors College

Abstract

Each day, antibiotic resistance affects the livelihood of individuals worldwide, especially in relation to hospital-acquired diseases. In an effort to combat this resistance, antimicrobial peptides, small biopolymers produced naturally by multicellular organisms, can be used to selectively eliminate bacteria and have demonstrated great potential as alternatives to conventional antibiotics. Many naturally-occurring antimicrobial peptides possess high concentrations of lysine and arginine amino acid residues, which are protonated and positively-charged at physiological pH. Herein, we describe the design and synthesis of antimicrobial peptide mimics, using amino acid mimics. N-3-aminopropyl methacrylamide (APMA) and 3-guanidinopropyl methacrylamide (GPMA) monomers mimic the amino acid residues lysine and arginine, respectively. Statistical copolymers of these two monomers were synthesized via aqueous reversible addition-fragmentation chain transfer (RAFT) polymerization and exhibited antimicrobial activity and low eukaryotic cell toxicity. To further analyze the mode of activity of these antimicrobial peptide mimics, large unilamellar vesicles (LUVs) containing fluorescent dye were prepared in an attempt to study the mechanisms of copolymer interactions with bacteria. . Developing a greater understanding of the relationship between the structure of synthetic antimicrobial peptide mimics and their respective mode of antimicrobial activity will aid in the design of tailored systems to target specific bacterial species.

Keywords: Antibiotic resistance; antimicrobial peptide mimics; polymers

Acknowledgements

I would like to thank my thesis advisor, Dr. Sarah Morgan, for mentoring me and providing me with much guidance throughout my college career. This work would also not have been possible without the expertise of Dr. Lea Paslay (a former graduate student in our lab) and Sarah Exley (a current graduate student in our lab). I would also like to thank our collaborators Brooks Abel (a graduate student in Dr. Charles McCormick's research group), Dr. Charles McCormick, Dr. Sabine Heinhorst, and Dr. Veena Choudhary.

This work was supported by the Department of Education Graduate Assistance in Areas of National Need (GAANN) Award # P200A120118 through the University of Southern Mississippi as well as the National Science Foundation International Research Experiences for Students Award No. OISE-1132079.

Table of Contents

List of Tables.....	viii
List of Figures.....	ix
List of Schemes.....	xi
Chapter I: Introduction.....	1
1.1. Prevalence of Antibiotic-Resistance Organisms.....	1
Chapter II: Literature Review of Antimicrobial Peptides and Synthetic Mimics.....	3
2.1. Antimicrobial Peptides.....	3
2.2. Synthetic Antimicrobial Peptide Mimics.....	5
Chapter III: Methodology.....	10
3.1 Research Goals and Objectives.....	10
3.2 Synthesis of Antimicrobial Peptide Mimics.....	10
3.2.1 Nuclear Magnetic Resonance (NMR) Spectroscopy.....	14
3.2.2 Aqueous Size Exclusion Chromatography.....	15
3.3 Quantification of Antimicrobial Activity.....	16
3.3.1 Broth Microdilution Method.....	16
3.3.2 Agar Plate Conformation of MIC.....	16
3.4 Assessment of Eukaryotic Biocompatibility.....	17
3.4.1 Hemolysis Studies.....	17
3.4.2 MTT Assay (Cell Viability).....	18
3.5 Determination of Prevailing Mode of Activity.....	19
Chapter IV: Results and Discussion.....	21
4.1 Monomer and Polymer Characterization.....	21

4.2 Antimicrobial Behavior.....	26
4.3 Hemolysis Studies.....	28
4.4 MTT Assay (Cell Viability).....	29
Chapter V: Conclusions.....	30
Chapter VI: Future Work.....	31
References.....	32

List of Tables

Table 1: Target molecular weight and copolymer composition data for proposed polymer systems.....	11
Table 2: Summary of molecular weight and composition data for synthesized homopolymers and copolymers.....	25
Table 3: Summary of broth microdilution testing of various polymers with bacteria as determined through optical density measurements.....	26

List of Figures

Figure 1: Structures of cationic amino acids lysine (A) and arginine (B), which are protonated at physiological pH (~7.4).....	2
Figure 2: The barrel-stave model of the AMPs biocidal mechanism.....	4
Figure 3: A variation of polynorbornene derivatives with differences in hydrophobicity to mimic AMPs.....	6
Figure 4: Varying the degree of lipophilic character on the pendant amine moiety for statistical copolymers.....	7
Figure 5: Polymer A ⁴ substituted with a guanidinium moiety (A). Polymer C ⁴ modified with variations in charge density (B).....	8
Figure 6: Structure of HPMA-b-GPMA block copolymer.....	9
Figure 7: Structures of N-3-aminopropyl methacrylamide (APMA) and 3-guanidinopropyl methacrylamide (GPMA).....	12
Figure 8: Avanti Polar Lipids, Inc. Mini-Extruder was used to form uniform vesicles with a 200 nm hydrodynamic radius.....	20
Figure 9: ¹ H NMR spectrum of boc-protected GPMA.....	21
Figure 10: ¹ H NMR spectrum of GPMA after boc-deprotection with TFA.....	22
Figure 11: APMA- <i>stat</i> -GPMA reaction kinetics. ln([M ₀]/[M]) versus time kinetic plot for the polymerization of 1:1 molar ratio of APMA:GPMA TFA.....	23
Figure 12: APMA- <i>stat</i> -GPMA molecular weight distribution as a function of reaction time.....	24
Figure 13: Representative ¹ H NMR spectrum of APMA- <i>stat</i> -GPMA copolymer.....	25

Figure 14: MIC agar plate confirmation.....	27
Figure 15: Polymers cause negligible hemolysis (<10 %) up to 3000 µg/mL.....	28
Figure 16: Cell viability of MCF-7 cells after incubation with polymers PAPMA, PGT 50, and PGT 100 for 6 and 12 hours.....	29

List of Schemes

Scheme 1: Synthesis of GPMA with TFA salt.....	13
Scheme 2: Statistical polymerization of APMA with GPMA via aqueous RAFT polymerization.....	14

Chapter I: Introduction

1.1 Prevalence of Antibiotic-Resistant Organisms

Over the past several decades, the increasing number of microorganisms resistant to traditional antibiotics has caused a growing concern for the well-being of individuals worldwide. A few examples of resistant bacteria include methicillin-resistant *Staphylococcus aureus* (MRSA), *Streptococcus pneumoniae*, and multidrug-resistant tuberculosis (MDR TB). The presence of resistant strains of bacteria leads to increased healthcare costs for possible treatments and an increase in the mortality rate of infected individuals. The amount of drug resistance can be attributed, at least in part, to the overuse of widely-available traditional antibiotics, which inadvertently promotes the presence of resistant pathogens and adaptive mutations.¹ In an effort to circumvent these and other severe bacterial infections, researchers have sought to exploit the benefits of naturally-occurring, antimicrobial peptides.²⁻⁶

Antimicrobial peptides (AMPs) are biological polymers, typically 20 to 50 amino acids in length, found in a variety of multicellular organisms. AMPs selectively target bacterial cells and induce cell death without causing harm to eukaryotic cells within a certain therapeutic concentration range.⁷ Because of the high concentrations of basic amino acids, such as lysine and arginine, found in these peptides, AMPs are generally positively-charged at physiological pH (**Figure 1**). Initial interactions between AMPs and bacteria are facilitated via electrostatic attraction due to the abundance of negatively-charged phospholipids in the cytoplasmic membrane of bacteria. In addition to these hydrophilic residues, AMPs also possess hydrophobic regions that can be inserted into the hydrophobic core of the membrane and induce cell death by

way of membrane disruption. In order for bacteria to develop resistance to these peptides, a drastic change in the bacterial cell membrane would have to occur.⁷

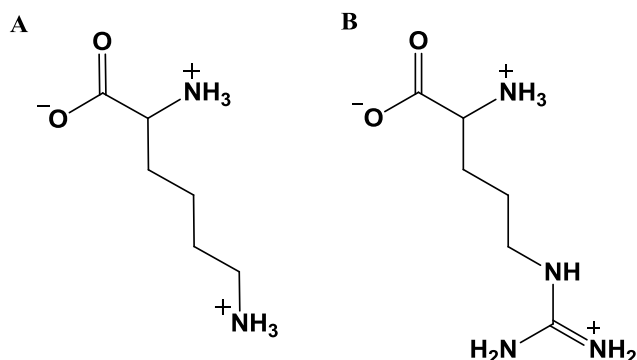


Figure 1. Structures of cationic amino acids lysine (A) and arginine (B), which are protonated at physiological pH (~7.4).

Although bacteria share similar structural features, varying membrane compositions can lead to differences in therapeutic susceptibility. Thus, certain bacterial species may be vulnerable only to particular AMPs or synthetic derivatives.⁸ Differences in vulnerability could be the result of the various modes in which the therapeutic agents induce cell death. Unfortunately, the mechanisms driving the activity of AMPs are quite complex and not fully understood due to the plethora of AMP structures, host biological composition, and other not-well defined variables.⁷ This research project aims to develop a better understanding of the factors that may affect the antimicrobial activity of AMPs by designing structures that mimic naturally, occurring AMPs and analyzing the respective modes of activity of these systems.

Chapter II: Literature Review of Antimicrobial Peptides and Synthetic Mimics

2.1 Antimicrobial Peptides

Antimicrobial peptides (AMPs) exhibit selective targeting and elimination of bacterial species over eukaryotic tissues. The preferred selection of prokaryotes is governed by electrostatic attraction between AMPs and bacterial cytoplasmic membranes at physiological pH (~7.4).⁷ AMPs possess high concentrations of the basic amino acids lysine and arginine, which are protonated and positively-charged at physiological pH. The outermost leaflet of prokaryotic cytoplasmic membranes is composed of negatively-charged phospholipid head groups, such as phosphatidylglycerol, cardiolipin, and phosphatidylserine.⁸ The electrostatic interactions between positively-charged AMPs and negatively-charged prokaryotic cell membranes mediate the initial, rapid targeting of the bacterial species. The speed at which this interaction occurs must be relatively fast in order to avoid renal excretion of the AMPs.⁹ Eukaryotic cell membranes, on the other hand, are populated with a majority of zwitterionic phospholipids, such as phosphatidylethanolamine, phosphatidylcholine, and sphingomyelin. Since they exhibit a net neutral charge, eukaryotic cells are less likely to be targeted by AMPs due to the limited electrostatic attraction.⁸ Cholesterol found in the lipid bilayer of eukaryotic membranes is also believed to either enhance the stability of the bilayer to AMP infiltration or aid in the deactivation of the AMP molecule before membrane disruption can occur.¹⁰

AMPs consist of approximately 50% hydrophobic residues, and their hydrophobic character is essential for inducing cell death. After the peptide is attracted to a phospholipid membrane, the hydrophobic portion of the peptide enters the hydrophobic core, causing the

integrity of the membrane to be compromised.¹¹ A schematic representation of one accepted mechanism for this process, known as membrane disruption, is depicted in **Figure 2**. Studies¹²⁻⁴ have shown that the selectivity of antimicrobial polymers towards prokaryotic cells over eukaryotic cells decreases with increases in available hydrophobic interactions. Thus, if the hydrophobicity of the compound is increased past a critical concentration, mammalian cell death will dramatically increase despite the presence of zwitterionic phospholipids and other compounds in the membrane. These studies¹²⁻⁴ suggest that an amphipathic balance of hydrophilicity and hydrophobicity must be maintained to minimize eukaryotic cell toxicity while maximizing antimicrobial efficiency.

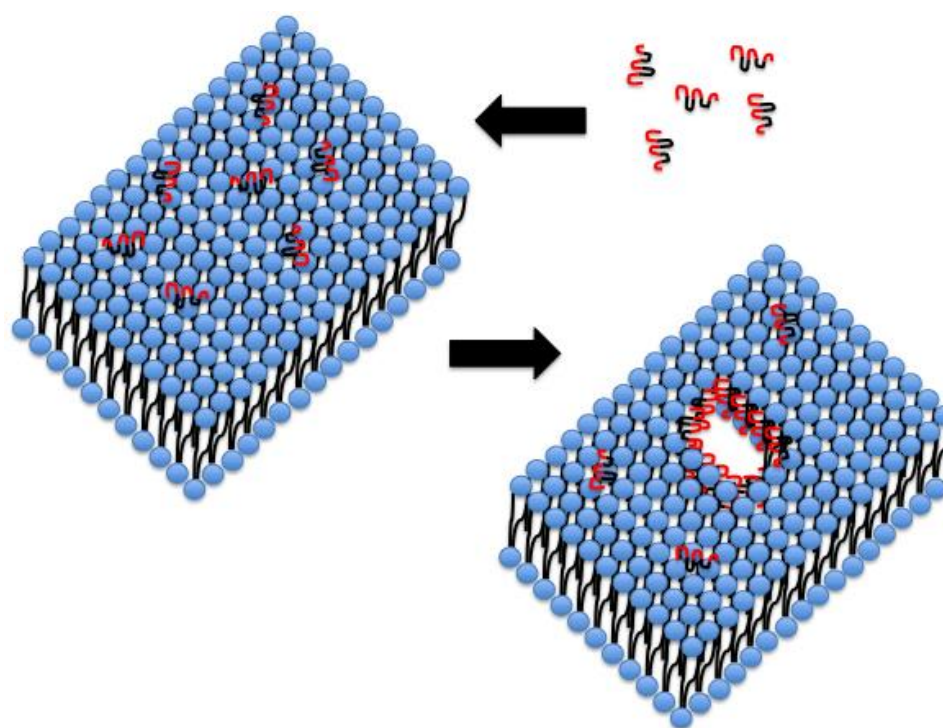


Figure 2. The barrel-stave model of the AMPs biocidal mechanism. Modified from Brogden et al.¹³ and extracted from Paslay et al.¹⁴

An alternative proposed mechanism of antimicrobial action involves AMPs permeation of the cell membrane of bacteria and binding to the negatively-charged nucleic acids in the cell, which leads to the inhibition of protein synthesis.¹⁵ Because AMPs interact with the phospholipid bilayer of the cytoplasmic membrane, bacterial cells are less likely to develop resistance to AMPs than to other conventional antibiotics that may only inhibit pathways that can develop resistance easily through mutations.⁸ A drastic change to the membrane composition is highly unlikely, which contributes to the difficulty in developing resistance.⁸ However, a limited number of organisms have been shown to develop resistance to naturally-occurring AMPs by altering the net charge of their outer surface, manipulating the proteins found in the membrane, and expressing genes for the production of proteolytic enzymes to degrade AMPs.¹³

Despite the specificity and therapeutic advantages of AMPs over conventional antibiotics, there are several disadvantages of using AMPs. Even though various multi-cellular organisms produce AMPs naturally, extraction procedures typically exhibit low yield. Furthermore, AMPs can be synthesized from individual amino acids; however, the production and purification costs for these compounds are quite high.¹⁰

2.2 Synthetic Antimicrobial Peptide Mimics

To compensate for the relatively low abundance and costly direct synthesis of AMPs, researchers have since attempted to find alternative routes of creating AMP mimics using synthetic methods.

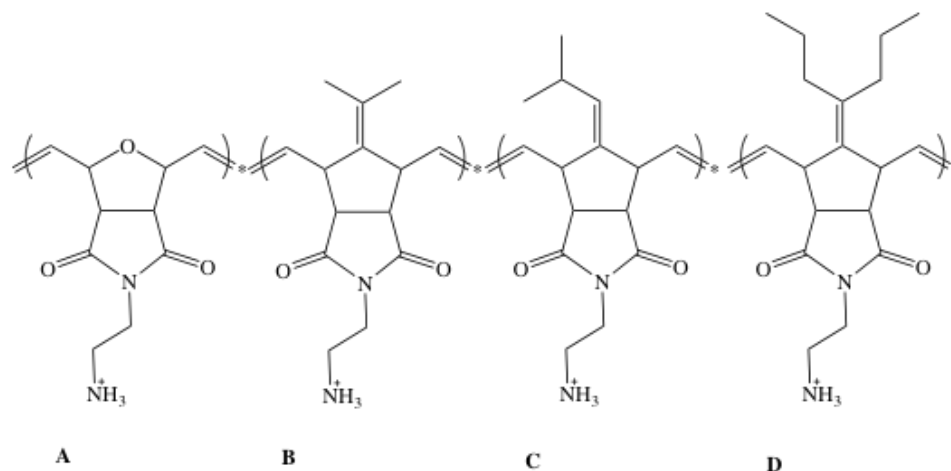


Figure 3. A variation of polynorbornene derivatives with differences in hydrophobicity to mimic AMPs.⁴

Utilizing ring opening metathesis polymerization (ROMP) with polynorbornene derivatives, Ilker et al.⁴ sought to mimic AMPs by forming homopolymers containing a pendant primary amine, characteristic of the amino acid lysine, shown in **Figure 3**. The protonated form of this pendant moiety mediates the binding of the polymers to the anionic phospholipid-rich surface of prokaryotic cells. Variation in relative hydrophobicity was obtained by changing the alkyl chain length and structure as shown in **Figure 3 A-D**. Antimicrobial studies showed polymer A, which had the least amount of hydrophobic character, was ineffective at eliminating bacteria. By increasing the hydrophobicity of the polymers, a general trend of increased antimicrobial activity and decreased selectivity was observed. Thus, Ilker and coworkers were able to manipulate the amphiphilic balance of the polymers using monomers with desired properties at various ratios to synthesize statistical copolymers.⁴ These polymers were found to induce prokaryotic cell death via a membrane disruption mechanism. The initial binding to the prokaryote was believed to be facilitated by the electrostatic interactions between the cationic polymers and the anionic phospholipid bilayer of bacterial membranes. The hydrophobic regions

of the polymers interacted with the hydrophobic core of the phospholipid bilayer, causing the cell to rupture.

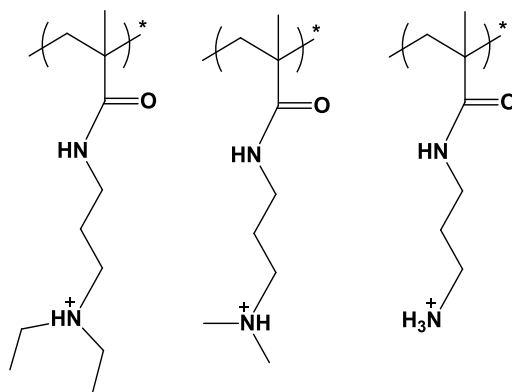


Figure 4. Varying the degree of lipophilic character on the pendant amine moiety for statistical copolymers.¹⁴

In previous studies in our laboratories (Paslay et al.¹⁴), we designed statistical copolymers via aqueous reversible addition-fragmentation chain-transfer (RAFT) polymerization using monomers with lysine-mimicking residues. The relative hydrophobic character of the monomers was altered by incorporating two methyl and two ethyl groups, respectively, as part of the pendant amine, as shown in **Figure 4**. Paslay et al. hypothesized that increasing the hydrophobicity would increase membrane activity towards bacteria, while the fully water-soluble nature of the amine species would reduce eukaryotic cell toxicity. While all the polymers displayed minimal eukaryotic toxicity, copolymers containing high concentrations of primary amine showed the highest levels of toxicity to both Gram-positive and Gram-negative bacteria.¹⁴

Gabriel et al.³ explored the possibility of incorporating a guanidinium moiety to alter the mode of cell death. The primary amine of polymer A, shown in **Figure 3**, was substituted with a guanidinium moiety, shown in **Figure 5A**, which mimics the amino acid arginine.³ Peptides rich in arginine have been shown to present cell penetrating behavior. There has been much research exploring various mechanisms in which these arginine-rich peptides are internalized by a cell.¹⁶

Upon internalization, this type of peptide has been shown to bind to negatively-charged nucleic acids and inhibit protein synthesis. These and other disruptions in cellular processes promote the inability of the cell to sustain life.¹⁵ While polymer A was ineffective in killing bacteria, upon the replacement of the primary amine with the guanidinium moiety for polymer A, Gabriel and coworkers showed that the polymer had selective antimicrobial activity without causing any observable prokaryotic membrane disruption.³

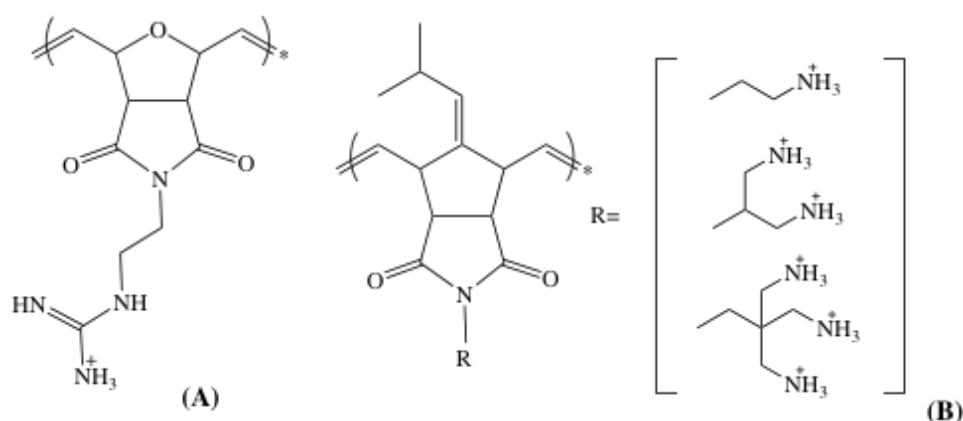


Figure 5. Polymer A⁴ (from **Figure 3**) substituted with a guanidinium moiety (A).³ Polymer C⁴ (from **Figure 3**) modified with variations in charge density (B).²

Al-Badri et al.² evaluated the effect of charge density on selectivity for synthetic AMP polynorbornene derivatives. Polymer C, shown in **Figure 3**, was modified by increasing the number of pendant primary amines from 1 to 3, as shown in **Figure 5B**. These systems showed a decrease in the hemolytic concentration (HC₅₀), or the minimum concentration required for 50% hemolysis of blood cells, changing from very hemolytic to (<1 µg/mL) to much less hemolytic (700 µg/mL). This suggests an increase in biocompatibility results with increased charge density

while maintaining the same relative antimicrobial efficiency reported for the original polymer. Further studies are needed to determine if there is a maximum amount of charge density where no improved selectivity would be observed.

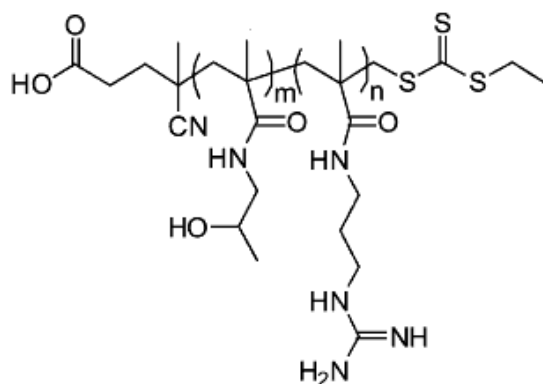


Figure 6. Structure of HPMA-b-GPMA block copolymer. Extracted from Treat et al.¹⁷

In a recent communication, Treat et al.¹⁷ report the synthesis of guanidinium-containing polymers via aqueous RAFT polymerization to mimic cell-penetrating peptides (**Figure 6**). 3-guanidinopropyl methacrylamide (GPMA) was copolymerized with N-(2-hydroxypropyl) methacrylamide (HPMA) to create block copolymers. The penetration of these polymers into KB cancer cells through endocytosis and non-endocytosis pathways was probed. Only the polymers containing the guanidinium moiety in this study were shown to penetrate the cell membrane. Polymers deficient in the guanidinium moiety did not penetrate the cell membrane. Antimicrobial activity and biocompatibility were not analyzed in this study.

The cell penetration behavior of AMPs mimics and the mechanism by which cell death is induced are not well understood. Because of the variable nature of bacterial species, prokaryotes do not all possess the same cell membrane composition, overall charge, expressed genes, and

many other characteristics. We hypothesize that structural variations in synthetic AMPs mimics, including charge density, molecular weight, hydrophobicity, and functional groups, have a direct relationship to antimicrobial activity towards bacteria of different structures. Developing a greater understanding of the relationship between AMPs structure and antimicrobial activity for bacterial species of different types will ultimately enable the design of systems to target specific prokaryotes based upon their structural features.

Chapter III: Methodology

3.1 Research Goals and Objectives

The purpose of this research is to design novel homopolymers and statistical copolymers that mimic antimicrobial peptides and to study their antimicrobial behavior in order to gain a better understanding of the relationship between structural components and mode of activity. The goals of this project can be outlined by three main objectives:

- 1) Evaluation of antimicrobial activity and hemolytic character of synthesized polymers to determine the relationship between activity and polymer composition.
- 2) Determination of the relationship between structural features of synthesized polymers, such as molecular weight and ionic character, and mechanism of activity.
- 3) Characterization of the selectivity of various homopolymer and copolymer systems towards a broad range of cell types, including Gram-positive bacteria, Gram-negative bacteria, red blood cells, and other complex eukaryotic cells.

3.2 Synthesis and Characterization of Antimicrobial Peptide Mimics

Two monomers, N-3-aminopropyl methacrylamide (APMA) and 3-guanidinopropyl methacrylamide (GPMA), were used to create homopolymers and statistical copolymers of varying copolymer compositions (**Table 1**). The nomenclature PGT represents polyGPMA TFA and the corresponding number indicates its targeted mole fraction (mol %) in the copolymer. For example PGT 25 represents a copolymer composed of 25 mol % GPMA TFA and 75 mol % APMA. The nomenclature Cl and TFA next to the polymer represent the counterion for APMA and GPMA, respectively.

Table 1. Target molecular weight and copolymer composition data for proposed polymer systems.

Polymer Label	Mol % GPMA (theory)	Mol % APMA (theory)	M _n (g/mol)
1 (PAPMA) (Cl)	0	100	5,600
2 (PGT 25) (TFA)	25	75	6,500
3 (PGT 50) (TFA)	50	50	7,400
4 (PGT 75) (TFA)	75	25	8,300
5 (PGT 100) (TFA)	100	0	9,200

APMA consists of a pendant primary amine moiety, similar to the amino acid lysine, and was commercially available. GPMA consists of a pendant guanidinium moiety, similar to the amino acid arginine (**Figure 7**).

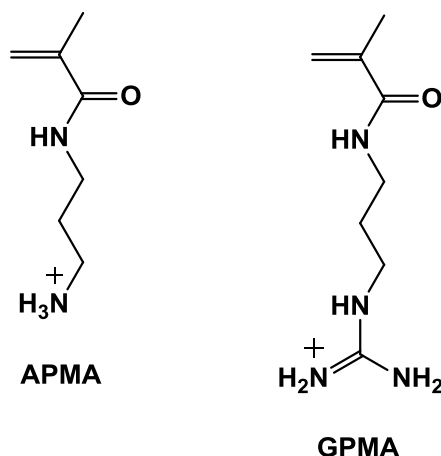
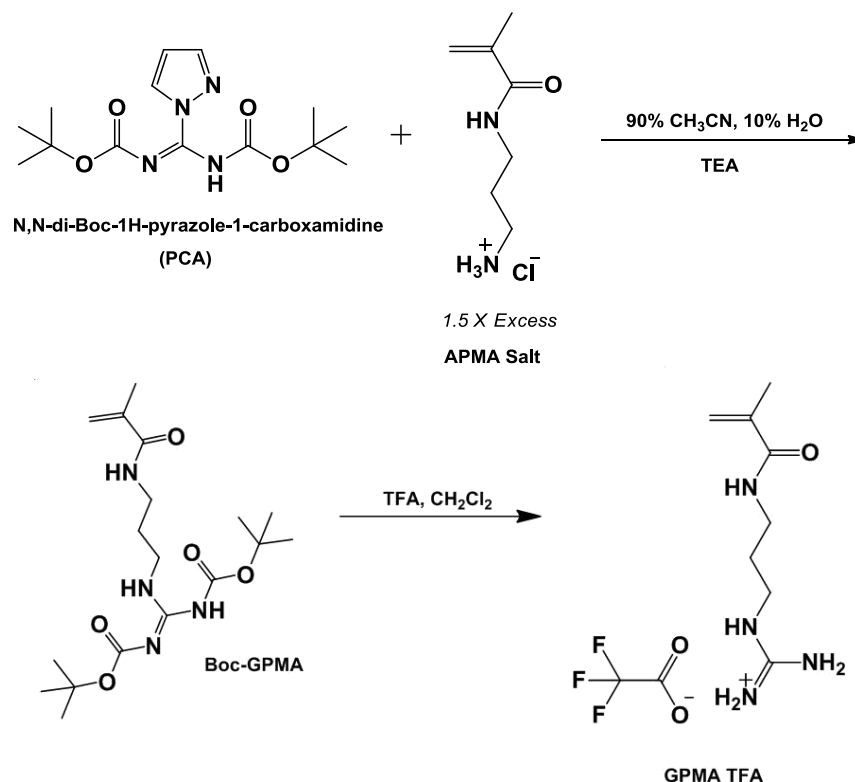


Figure 7. Structures of N-3-aminopropyl methacrylamide (APMA) and 3-guanidinopropyl methacrylamide (GPMA).

Since GPMA is not commercially available, this monomer was synthesized (**Scheme 1**). In a 250 mL round bottom flask, APMA HCl was dissolved in a mixture of 12 mL DI H₂O and 20 mL (148 mmol) TEA and stirred at 25°C. 10 g (32 mmol) N,N'-di-boc-1H-pyrazole-1-carboxamidine (PCA) was dissolved in 108 mL acetonitrile and added dropwise to the stirring APMA solution via an addition funnel over the course of 30 min. The reaction progressed for 24 hours. The product was obtained via filtration and then washed 3 times with 50 mL DI water (yield = 91%).

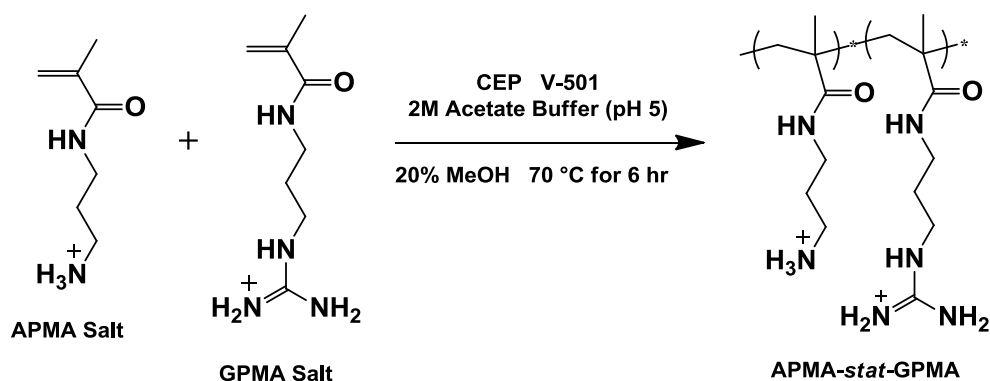
In a 250 mL round bottom flask, 10.96 g (28.48 mmol) boc-protected GPMA was dissolved in 87 mL CH₂Cl₂ stirring at 0°C. 87 mL (1.14 mol) (20 equivalences per boc-protecting group) trifluoroacetic acid (TFA) was then added to the solution dropwise via an addition funnel and the reaction was allowed to progress for 16 hours warming from 0°C to 25°C. The solvents were removed via rotary evaporation and the resulting clear viscous oil was dissolved in 250 mL DI H₂O, frozen in liquid N₂ and lyophilized for 48 hours. The product was obtained as a white solid.



Scheme 1. Synthesis of GPMA with TFA salt.

The polymerizations were accomplished via aqueous reversible addition chain transfer fragmentation (RAFT) techniques. Polymer molecular weights were targeted by selecting appropriate initial monomer and CTA concentrations. The ratio of the initial monomer concentration (M_0) to the initial chain transfer agent concentration (CTA_0) was set to be approximately 30:1 to yield a degree of polymerization of approximately 30, which mimics the size of naturally occurring AMPs. 4-cyano-4-(ethylsulfanylthiocarbonylsulfanyl)pentanoic acid (CEP) was used as the CTA and was synthesized via previously published procedures,¹⁸ while 4,4'-Azobis(4-cyanopentanoic acid) was used as the initiator. For all polymerizations, the CTA_0 was five times more than the initial initiator concentration (I_0). The polymerization took place in aqueous 2 M acetate buffer (pH 5) at 70 °C¹⁹ for 6 hours (**See Scheme 2**). Methanol was added in low quantities (20%) to improve the solubility of CEP in the aqueous media. After the

reactions were completed the solutions were exposed to air and quenched in liquid nitrogen. The solutions were then dialyzed against water for 72 hours followed by lyophilization for 72 hours and the samples were then stored in desiccant. A representative yield was calculated to be 75% of the theoretical yield. Some polymer is lost in dialysis due to excessive swelling of the dialysis tubing as a result of internal osmotic pressure. This loss can be minimized by making the water slightly acidic during the dialysis procedure to reduce the extent of swelling.



Scheme 2. Statistical polymerization of APMA with GPMA via aqueous RAFT polymerization.

3.2.1 Nuclear Magnetic Resonance (NMR) Spectroscopy

Proton (^1H) NMR was performed with a Varian Mercury^{PLUS} 300 MHz spectrometer in deuterated chloroform (CDCl_3), utilizing delay times of 5 s to determine monomer purity. A 500 MHz NMR equipped with a standard 5 mm proton and carbon-13 ($^1\text{H}/^{13}\text{C}$) probe and operating at 499.77 MHz (^1H) was used to confirm the synthesis of the GPMA monomer, identify the homopolymer structures of PAPMA and PGT 100, and identify the statistical structures of PGT

25, PGT 50, and PGT 75 copolymers in deuterium oxide (D₂O). 64 scans were taken for each experiment with a 3.1 second recycle delay.

3.2.2 Aqueous Size Exclusion Chromatography

The molecular weight and polydispersity index (PDI) of the polymers were determined by aqueous size exclusion chromatography (ASEC) coupled with multi-angle laser light scattering (MALLS). Eprogen CATSEC columns (100, 300 and 1000 Å) were used in combination with a Wyatt Optilab DSP interferometric refractometer ($k = 690$ nm) and a Wyatt DAWN DSP MALLS detector ($k = 633$ nm). Acetic acid (1 weight %) and 0.1 M sodium sulfate (Na₂SO₄) (aqueous) was used as the eluent at a flow rate of 0.25 mL/min. The interferometric refractometer was utilized off-line to determine dn/dc values for PAPMA at 25 °C in the eluent (0.2000 mL/g) in order to assign absolute molecular weight values to all polymers. For the statistical polymers the dn/dc values were calculated as the mole fraction-averaged composites of the measured homopolymer dn/dc values using the copolymer compositions determined by NMR spectroscopy. Wyatt ASTRA size exclusion chromatography/light scattering (SEC/LS) software was used for molecular weight and PDI calculations.

3.3 Quantification of Antimicrobial Activity

3.3.1 Broth Microdilution Method

Antimicrobial efficiency of the polymers was assessed using *Bacillus subtilis* (19659), *Staphylococcus aureus* (both Gram-positive bacteria), and *Escherichia coli* (DH5 α) (Gram-negative bacteria) following a modified version of a previously published procedure.³ Stock solutions of both bacterial species were grown at 37°C in inoculated Luria broths (LB) overnight while undergoing agitation. Concentrations of 4 to 6 mg/mL polymer stock solutions were prepared in tris(hydroxymethyl)aminomethane (TRIS) buffered saline (TBS) (10 mM TRIS, 150 mM NaCl) (pH 7.4). In a 96 well plate, varying buffered polymer dilutions were mixed 1:1 with bacterial cultures that have been diluted with fresh LB to an optical density (OD) of 0.001 at 600 nm (OD₆₀₀). Over a 24-hour period, these mixtures were incubated at 37°C with agitation. The OD₆₀₀ was determined using to a UV-Visible plate reader after incubations. Minimum inhibitory concentrations (MIC) were reported at multiple time intervals as the polymer concentrations that inhibit 90% of bacterial growth.

3.3.2 Agar Plate Conformation of MIC

To confirm the MIC measurements from the broth microdilution experiments, the polymer concentrations above and below the MIC were inoculated with the respective bacterial species (*B. subtilis*, *S. aureus*, or *E. coli*) for 24 hours at 37°C with agitation. Inoculums were streaked onto sterile LB agar plates and incubated for an additional 18 hours at 37°C to allow for

any prevailing bacterial growth. If any living bacteria remained after incubation, bacterial colonies were visible on the agar plates. The absence of bacterial growth at the respective polymer concentrations confirmed the previously determined MIC.

3.4 Assessment of Eukaryotic Biocompatibility

3.4.1 Hemolysis Studies

Hemolysis experiments were performed according to a modified version of a previously published procedure.⁴ Red blood cells (RBCs) were separated from whole human blood by centrifugation at 1500 rpm for 10 minutes. RBCs (30 μ L) were suspended in 10 mL of buffer (TBS at a pH of 7.4), rinsed 3 times by centrifugation (10 min at 1500 rpm) and then re-suspended in 10 mL TBS. Polymers were dissolved in TBS to create 6.0 mg/mL stock solutions. These solutions were diluted to 0.1, 0.2, 2.0, 4.0 and 6.0 mg/mL. RBC suspensions were incubated 1:1 at 37 °C with light agitation for 30 min with polymer dilutions in microcentrifuge tubes to obtain final polymer concentrations of 0.05, 0.1, 1.0, 2.0 and 3.0 mg/mL. After incubation, the tubes were centrifuged at 1500 rpm for 10 min. The supernatant from each tube was transferred to individual wells in a 96 well plate and the absorbance was measured at 540 nm. Positive and negative controls for 100 and 0% hemolysis were obtained with 1% Triton-X and TBS, respectively.

3.4.2 MTT Assay (*Cell Viability*)

Methyl thiazol tetrazolium (MTT) assay were performed with MCF-7 cell lines using a modified version of a previously published procedure.²⁰ Cells were cultured on tissue culture polystyrene flacon flasks in Dulbecco's Modified Eagle's Medium (DMEM) supplemented with 10% fetal calf serum and 1% antibiotic solution (penicillin and streptomycin) at 37 °C in a 5% CO₂ incubator. After obtaining approximately 80% confluence the cells were trypsinized and counted on a hemocytometer. The cells in fresh media were placed into a 96 well plate (8x10³ cells/well) and incubated for 24 hours at 37 °C in a 5% CO₂ incubator. Next, the media was removed from each well and 100 µL of fresh media was added. To select wells (in triplicate) 50 µL of polymer solutions were added at various concentrations (90, 225, 375, and 6000 µg/mL). The resulting solutions had final polymer concentrations of 30, 75, 125, and 2000 µg/mL, respectively. For a positive control, 50 µL TBS (pH 7.4) was used, while 50 µL 3% Triton-X was used as a negative control. Reported data was normalized for viability observed in the positive control (taken as 100% viability). The plate was incubated for 6 or 12 hours at 37 °C in a 5% CO₂ incubator. After incubation, the media was removed from each well and 100 µL of fresh media was added. Next, 10 µL of MTT reagent (MTT dissolved in TBS at 5 mg/mL concentration) was added to each well and samples were incubated for an additional 4 hours. The media from each well was then removed and replaced with 100 µL of DMSO to solubilize the formed formazan crystals. Absorbance readings at 570 nm were recorded using a UV-Visible plate reader.

3.5 Determination of Prevailing Mode of Activity

Large unilamellar vesicles (LUVs) were prepared according to a modified version of a previously published procedure to determine mode of polymer activity.³ A solution of zwitterionic lipids 1-palmitoyl-2-oleoyl-sn-glycero-3-phospho-ethanolamine (POPE) (3.42 mg, 0.0045 mmol) and the anionic lipids 1-palmitoyl-2-oleoyl-phosphatidylglycerol (POPG) (1.15 mg, 0.0015 mmol) were mixed in a 3:1 ratio with 10 mL of chloroform in a 50 mL round-bottom flask, mimicking the composition of bacterial cell membranes. The solvent was removed at room temperature using a rotary evaporator to form a uniform film in the round-bottom flask. To remove any residual solvent, the flask was placed under vacuum for an additional 8 hours. A 40 mM calcein solution (aqueous) was prepared using a buffer (TBS at a pH of 7.4) as the solvent. The calcein dye solution was adjusted to an approximate pH of 7. The dry lipid film was then hydrated with 1.5 mL of the 40 mM calcein solution. The lipid and calcein mixture was subjected to five freeze/thaw cycles (5 minutes each) using liquid nitrogen and warm water, consecutively. Two stacked 200 nm porous polycarbonate membranes were heated to 40°C before the entire volume of the mixture was subjected to extrusion for a total of 20 passes (**Figure 8**). The mixture was then removed from the extrusion apparatus and allowed to equilibrate to room temperature before being passed through a Sephadex-25 column to remove residual calcein dye. Fractions of approximately 5 drops each were collected in Eppendorf microcentrifuge tubes. The vesicle solutions were stored at 4°C and diluted as needed for up to 4 days.



Figure 8. Avanti Polar Lipids, Inc. Mini-Extruder was used to form uniform vesicles with a 200 nm hydrodynamic radius.²¹

After the collection of the fractions, the hydrodynamic radius of the artificial vesicles was analyzed and confirmed to be 200 nm using dynamic light scattering. UV-Vis spectroscopy was used to determine the proper vesicle concentration to use for the LUV experiments. For this, 0.4 weight % Triton-X was added to the vesicle solution and the vesicle dilution for which the absorbance was less than 0.01 absorbance units for the UV-Vis experiment was recorded and used for the subsequent LUV studies. The average MIC of polymers (70 $\mu\text{g/mL}$) was used as the respective polymer concentration for the LUV studies. The percentage dye leakage was recorded as a function of time with a fluorometer after allowing 1 minute for the system to equilibrate per sample. The amount of dye released from the LUVs was evaluated to determine the mechanism of cell death, with a large release amount indicating cell death via a membrane disruption mechanism, while a small release amount indicates a membrane penetration mechanism of action of the polymers.

Chapter IV: Results and Discussion

4.1 Monomer and Polymer Characterization

As described in detail previously, the NMR spectra were collected for the boc-protected GPMA (**Figure 9**) and the final boc-deprotected GPMA salt (**Figure 10**). Most notable in **Figure 9** is the presence of the tert-butyl ester protecting group (~1.5 ppm) from the reaction with PCA. Upon deprotection with TFA, the signal peak at ~1.5 ppm disappears and the amine protons of the guanidinium moiety become noticeably present from ~7.0 to 8.0 ppm in **Figure 10**.

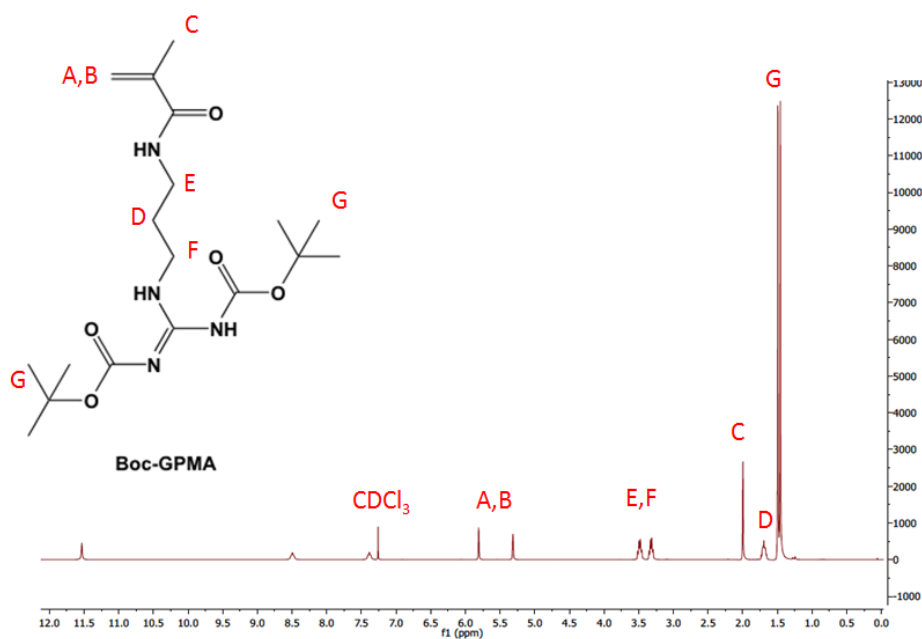


Figure 9. ^1H NMR spectrum of boc-protected GPMA.

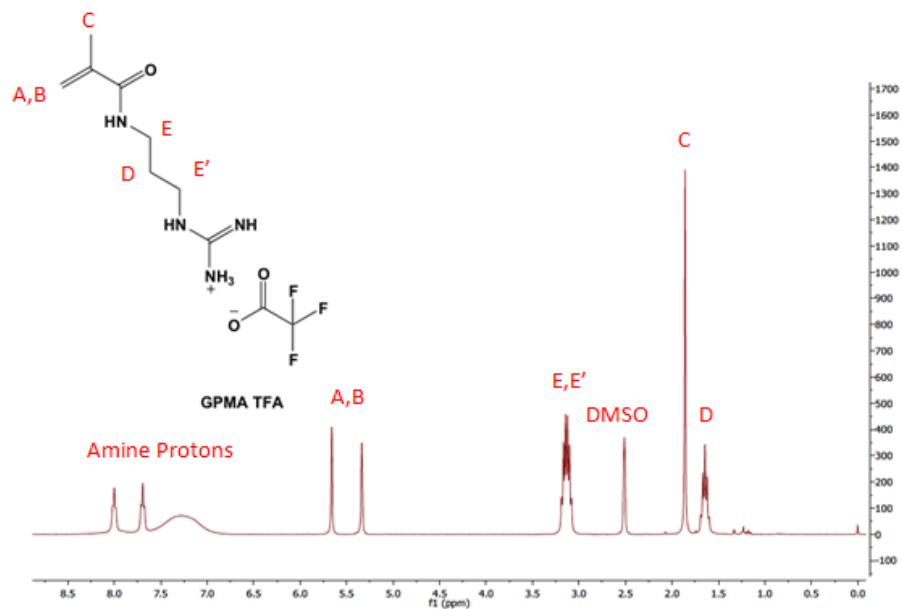


Figure 10. ^1H NMR spectrum of GPMA after boc-deprotection with TFA.

During the aqueous RAFT polymerization process, the reaction progress of APMA-*stat*-GPMA was monitored by taking aliquots every hour from the PGT 50 reaction vial. ^1H NMR was utilized to determine the monomer concentration $[\text{M}]$ at time (t) by comparing the vinylic hydrogen peak integrations to the integration of an internal standard, methanol (MeOH). A plot of $\ln([\text{M}_0]/[\text{M}])$ versus time indicates that the reaction follows linear pseudo first-order reaction kinetics (**Figure 11**).

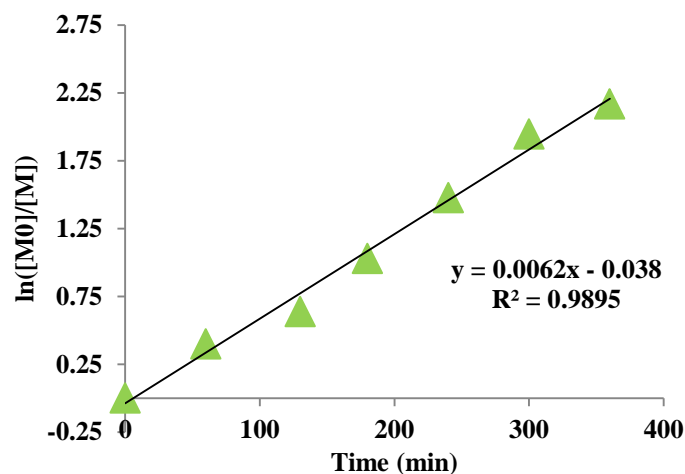


Figure 11. APMA-*stat*-GPMA reaction kinetics. $\ln([M_0]/[M])$ versus time kinetic plot for the polymerization of 1:1 molar ratio of APMA:GPMA TFA. The linear relationship indicates that the polymerization follows a predictable first-order reaction behavior typical of aqueous RAFT polymerizations.

Aqueous size exclusion chromatography (ASEC) coupled with multi-angle laser light scattering (MALLS) was utilized to monitor molecular weight as a function of time. The refractive index (RI) response versus elution volume for aliquots taken at each time interval is shown in **Figure 13**. As shown in this graph, the polymer molecular weight increases over time. The narrowing of the peak is indicative of a narrowing PDI over time.

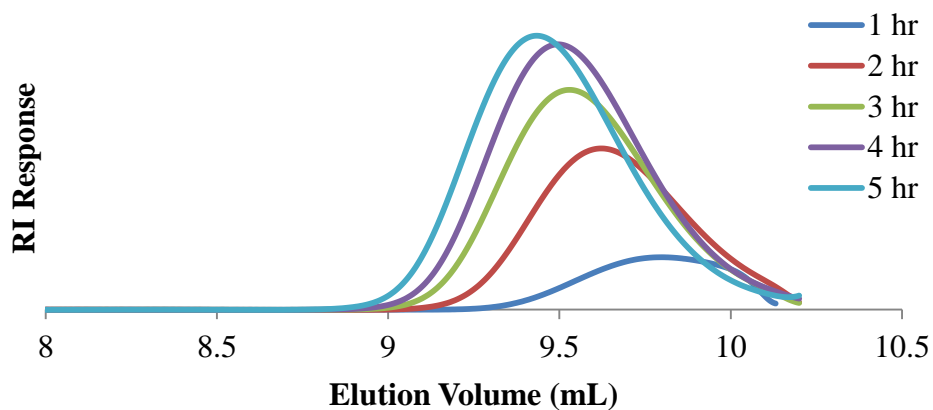


Figure 12. APMA-*stat*-GPMA molecular weight distribution as a function of reaction time. RI response versus elution volume at multiple time intervals during the polymerization reaction.

For each of the polymers, unique peak assignments were made, and the copolymer compositions were calculated for the statistical polymers via peak integration (**Figure 13**). A summary of molecular weight characterization data is provided in **Table 2**.

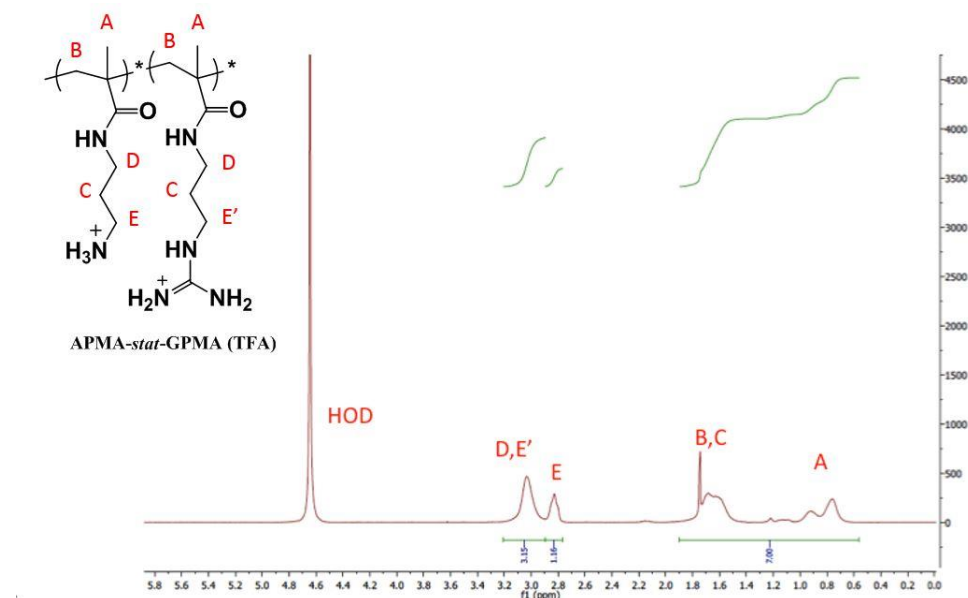


Figure 13. Representative ^1H NMR spectrum of APMA-*stat*-GPMA copolymer. The target APMA/GPMA composition for the above formulation was 50:50 mol %. Peak integration indicates 45 mol % GPMA in the copolymer.

Table 2. Summary of molecular weight and composition data for synthesized homopolymers and copolymers.

Polymer Label	Mol % GPMA (theory)	Mol % GPMA (exp) ^a	Mn, _{th} (g/mol) ^b	Mn, _{exp} (g/mol) ^c	PDI ^c	dn/dc ^d
1 (PAPMA) (Cl)	0	0	5,600	6,500	1.06	0.200
2 (PGT 25) (TFA)	25	23	6,500	6,900	1.03	0.183
3 (PGT 50) (TFA)	50	45	7,400	6,100	1.06	0.169
4 (PGT 75) (TFA)	75	72	8,300	5,800	1.12	0.152
5 (PGT 100) (TFA)	100	100	9,200	8,100	1.04	0.132

^aDetermined by ^1H NMR. ^bBased on 90% conversion of $[\text{M}_0]$. ^cDetermined by ASEC-MALLS. ^dDetermined by a Wyatt Optilab DSP interferometric refractometer.

4.2 Antimicrobial Behavior

The minimum inhibitory concentrations (MIC) were determined for each polymer for each of the three bacteria types (*B. subtilis*, *S. aureus*, and *E. coli*). The findings of these experiments are summarized in **Table 3**.

Table 3. Summary of broth microdilution testing of various polymers with bacteria as determined through optical density measurements.

Minimum Inhibitory Concentration (MIC) ($\mu\text{g/mL}$) ^a			
Polymer Label	<i>B. subtilis</i> ^b (19659)	<i>S. aureus</i> ^b	<i>E. coli</i> (DH5 α) ^c
1 (PAPMA) (Cl)	< 25	~ 300	\geq 300
2 (PGT 25) (TFA)	< 25	~ 300	70 - 300
3 (PGT 50) (TFA)	< 25	~ 300	70 - 300
4 (PGT 75) (TFA)	< 25	~ 300	~ 70
5 (PGT 100) (TFA)	< 25	~ 300	~ 70

^aDetermined by broth microdilution testing.

^bGram (+) bacteria. ^cGram (-) bacteria.

To validate the MIC measurements obtained from the broth microdilution testing, the polymer concentrations above and below the MIC were inoculated with the respective bacterial species (*B. subtilis*, *S. aureus*, or *E. coli*), streaked onto agar plates and allowed to grow. As shown in **Figure 14**, the inoculums grown on the agar plates confirmed the MIC values obtained from the broth microdilution testing.

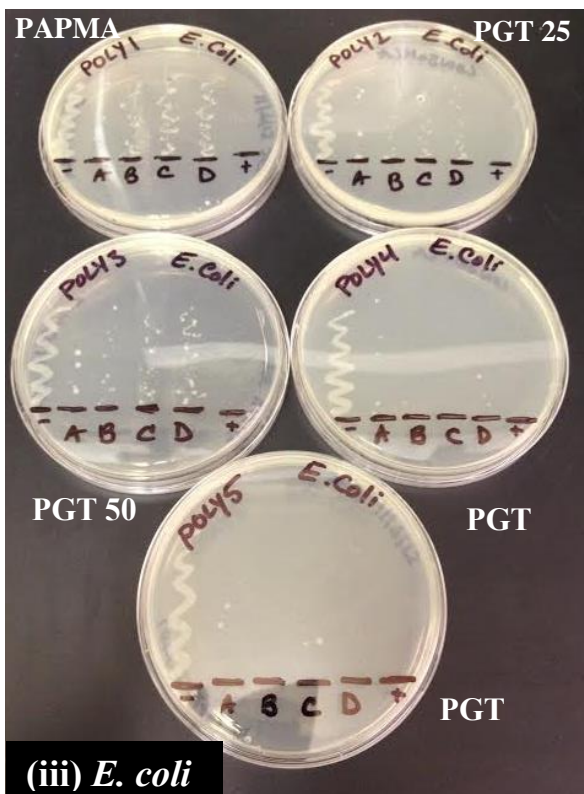
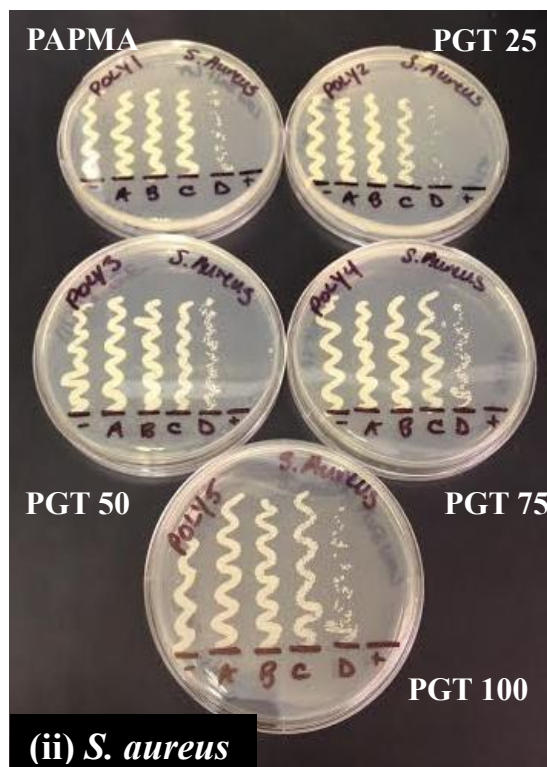
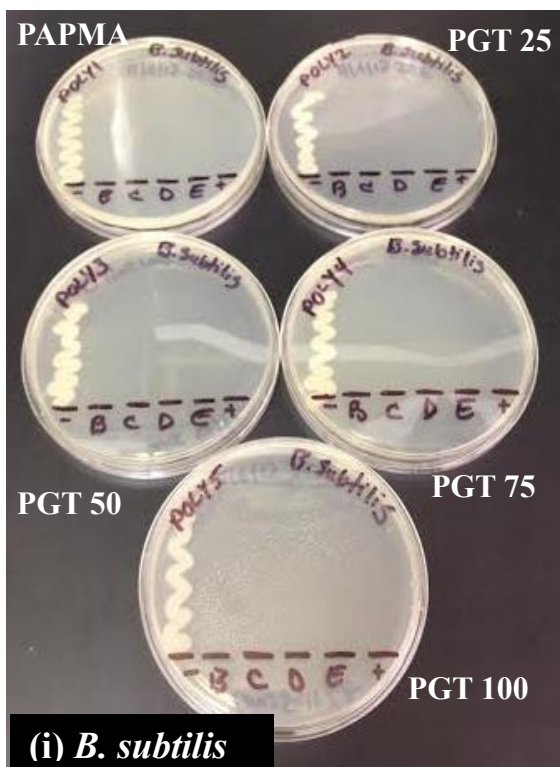


Figure 14. MIC agar plate confirmation. All agar plates consisted of a negative control (-) where only bacteria and no polymers were present along with a positive control (+) where only polymers and no bacteria were present. (i) *B. subtilis* with polymer concentration ranges of 25 (B), 50 (C), 70 (D), and 80 (E) $\mu\text{g/mL}$. (ii) *S. aureus* with polymer concentration ranges of 70 (A), 150 (B), 230 (C), and 300 (D) $\mu\text{g/mL}$. (iii) *E. coli* with polymer concentration ranges of 70 (A), 150 (B), 230 (C), and 300 (D) $\mu\text{g/mL}$.

4.3 Hemolysis Studies

An effective way to test eukaryotic cell toxicity is to study the hemolytic behavior of a system. While not conclusive, hemolysis experiments are used to indicate the possibility of eukaryotic cell toxicity. Less than 10 % hemolysis was observed for all polymer types, even at high concentrations (3,000 $\mu\text{g/mL}$). With increasing polymer concentration the percentage of red blood cells that lyse should either remain the same or increase, and within experimental error (as observed by the relatively high standard deviations observed) this trend was observed. .

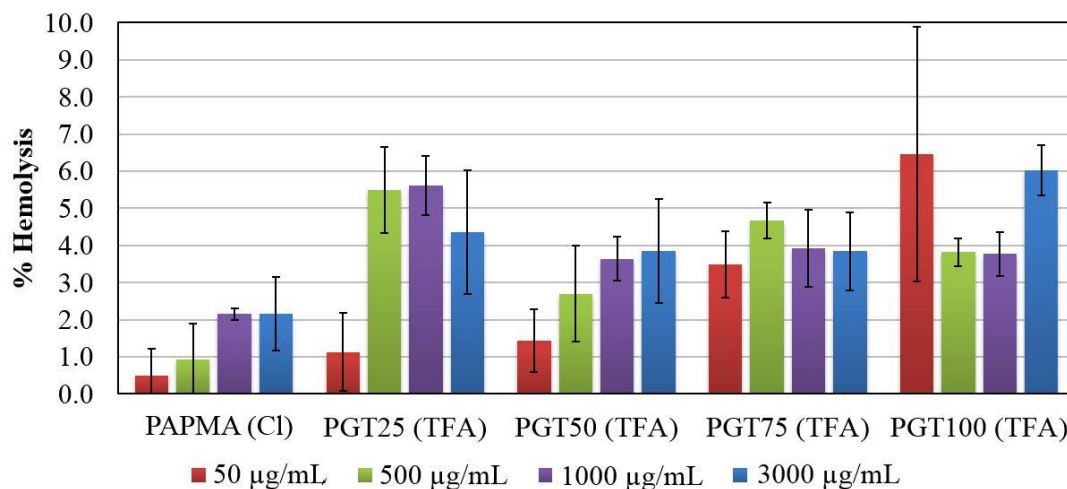


Figure 15. Polymers cause negligible hemolysis (<10 %) up to 3000 $\mu\text{g/mL}$. The concentration of polymer required to cause 50 % hemolysis (HC_{50}) is reported as >3000 $\mu\text{g/mL}$ to estimate polymer selectivity.

4.4 MTT Assay (Cell Viability)

MTT assays were performed to further investigate the eukaryotic cytotoxicity of the homopolymers of APMA and GPMA and the statistical copolymer PGT 50. **Figure 16** shows cell viability as a function of polymer concentration after 6 and 12 hours for these polymers. In a MTT assay, the conversion of MTT to purple formazan by mitochondrial reductase is utilized to quantify the mitochondrial activity of the cells rather than directly visualizing the number of living cells. Although the homopolymer of GPMA (PGT 100) caused negligible hemolysis, a drastic reduction in MCF-7 cell viability was observed at high concentrations ($>200 \mu\text{g/mL}$). However, this concentration is much higher than that required for antimicrobial effectiveness, ($\sim 70 \mu\text{g/mL}$).

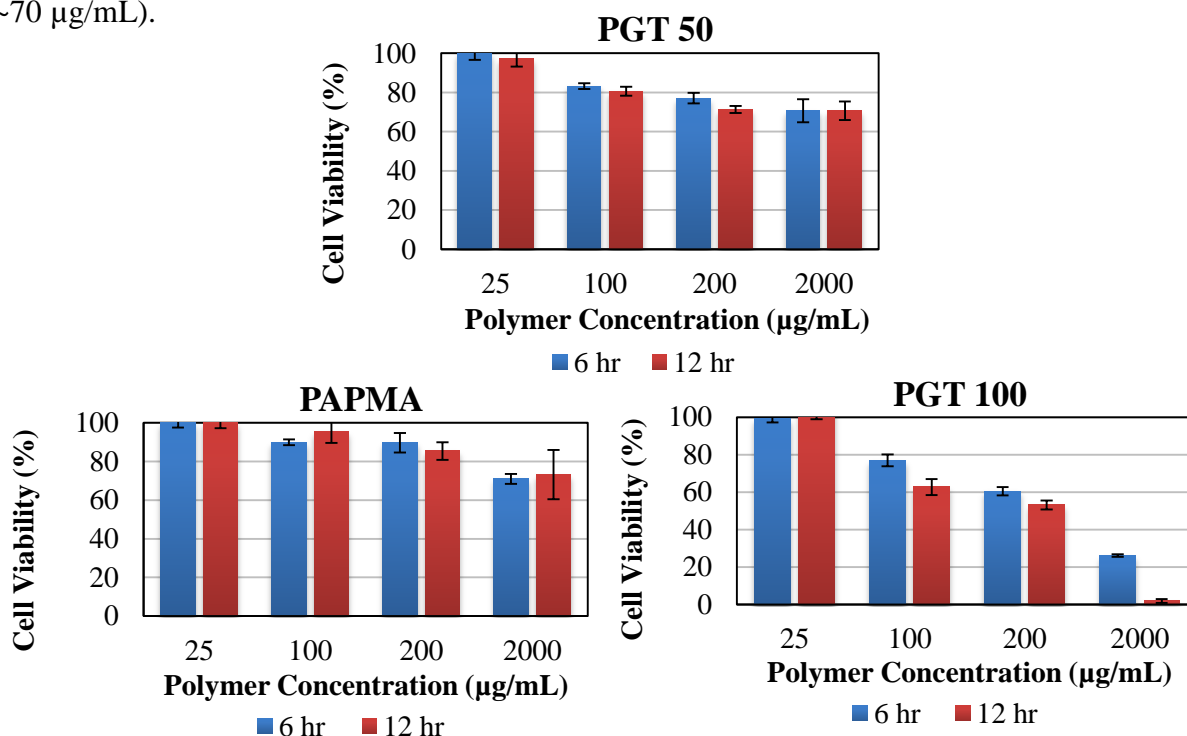


Figure 16. Cell viability of MCF-7 cells after incubation with polymers PAPMA (bottom left), PGT 50 (top), and PGT 100 (bottom right) for 6 and 12 hours.

Chapter V: Conclusions

A series of well-defined primary amine-functionalized and guanidinium-functionalized methacrylamide homopolymers and statistical copolymers were synthesized via aqueous RAFT polymerization. These polymeric mimics of antimicrobial peptides were all shown to exhibit excellent antimicrobial behavior (MICs of ~ 300 $\mu\text{g/mL}$ or lower) for *B. subtilis*, *S. aureus*, and *E. coli*. With *B. subtilis* and *S. aureus*, the MICs of the AMP mimics appeared to be the same for all polymer types of the respective bacteria. However with *E. coli*, increasing the guanidinium content greatly enhanced the antimicrobial efficiency of the polymer. Thus, the polymer structure, such as the presence of a primary amine and/or guanidinium moiety, appears to play a crucial role in its antimicrobial activity.

As shown in the biocompatibility studies (hemolysis experiments and MTT assays), these AMP mimics were shown to be selective for bacterial cells within the respective therapeutic range. However, the homopolymer of GPMA (PGT 100) was shown to drastically reduce cell viability at relatively high concentrations (>200 $\mu\text{g/mL}$). This trend, which did not appear in the cell viability trends of PAPMA or PGT 50, is most likely the result of a change in the mechanism of activity. Copolymers with high concentrations of guanidinium have been previously shown to follow a primarily membrane permeation mechanism, and this would explain the increased antimicrobial behavior and decreased cell viability at high concentrations.²² At high concentrations of the guanidinium moiety, loss of selectivity may occur due to the change in the mechanism of activity.

After several attempts to perform the large unilamellar vesicles (LUV) studies, the data gathered was not consistent and will not be provided in this report. The delicate nature of the

LUVs along with a high degree of experimental error yielded no reproducible data. Because negligible hemolysis was observed for all polymer compositions, it is concluded that the cell permeation mechanism was the dominant mode of antimicrobial activity for the polymers tested. Further investigation, including LUV experiments, is needed to substantiate this claim.

Chapter VI: Future Work

Antimicrobial peptide (AMP) mimics have been shown to be a promising alternative for conventional antibiotics against antibiotic-resistant microbes. It is recommended that LUV studies be performed with the antimicrobial peptide mimics described in this study. Elucidating the mechanism of action of these polymers will help to provide a better understanding of the structure-activity relationships present in these compounds. Once a suggested mechanism of action is proposed from the LUV studies, transmission electron microscopy imaging should be performed to further validate the proposed mechanism of action. This knowledge will be beneficial in designing new antimicrobial peptide mimics to target specific antibiotic-resistant bacteria in the future.

References

1. Levy, S. B.; Marshall, B., Antibacterial resistance worldwide: causes, challenges and responses. *Nature medicine* **2004**, *10*, S122-S129.
2. Al-Badri, Z. M.; Som, A.; Lyon, S.; Nelson, C. F.; Nüsslein, K.; Tew, G. N., Investigating the Effect of Increasing Charge Density on the Hemolytic Activity of Synthetic Antimicrobial Polymers. *Biomacromolecules* **2008**, *9* (10), 2805-2810.
3. Gabriel, G. J.; Madkour, A. E.; Dabkowski, J. M.; Nelson, C. F.; Nüsslein, K.; Tew, G. N., Synthetic Mimic of Antimicrobial Peptide with Nonmembrane-Disrupting Antibacterial Properties. *Biomacromolecules* **2008**, *9* (11), 2980-2983.
4. Ilker, M. F.; Nüsslein, K.; Tew, G. N.; Coughlin, E. B., Tuning the Hemolytic and Antibacterial Activities of Amphiphilic Polynorbornene Derivatives. *Journal of the American Chemical Society* **2004**, *126* (48), 15870-15875.
5. Paslay, L. C.; Abel, B. A.; Brown, T. D.; Koul, V.; Choudhary, V.; McCormick, C. L.; Morgan, S. E., Antimicrobial Poly(methacrylamide) Derivatives Prepared via Aqueous RAFT Polymerization Exhibit Biocidal Efficiency Dependent upon Cation Structure. *Biomacromolecules* **2012**, *13* (8), 2472-2482.
6. Scott, R. W.; DeGrado, W. F.; Tew, G. N., De novo designed synthetic mimics of antimicrobial peptides. *Current Opinion in Biotechnology* **2008**, *19* (6), 620-627.
7. Zasloff, M., Antimicrobial peptides of multicellular organisms. *Nature* **2002**, *415* (6870), 389-395.
8. Yeaman, M. R.; Yount, N. Y., Mechanisms of antimicrobial peptide action and resistance. *Pharmacol. Rev.* **2003**, *55*, 27-55.

9. Welling, M. M.; Paulusma-Annema, A.; Balter, H. S.; Pauwels, E. K. J.; Nibbering, P. H., Technetium-99m labelled antimicrobial peptides discriminate between bacterial infections and sterile inflammations. *Eur. J. Nucl. Med.* **2000**, 27, 292-301.
10. Rotem, S.; Mor, A., Antimicrobial peptide mimics for improved therapeutic properties. *Biochimica et Biophysica Acta (BBA)-Biomembranes* **2009**, 1788 (8), 1582-1592.
11. Wieprecht, T.; Dathe, M.; Beyermann, M.; Krause, E.; Maloy, W. L.; MacDonald, D. L.; Bienert, M., Peptide Hydrophobicity Controls the Activity and Selectivity of Magainin 2 Amide in Interaction with Membranes. *Biochemistry* **1997**, 36 (20), 6124-6132.
12. Eren, T.; Som, A.; Rennie, J. R.; Nelson, C. F.; Urgina, Y.; Nüsslein, K.; Coughlin, E. B.; Tew, G. N., Antibacterial and Hemolytic Activities of Quaternary Pyridinium Functionalized Polynorbornenes. *Macromolecular Chemistry and Physics* **2008**, 209 (5), 516-524.
13. Brogden, K. A., Antimicrobial peptides: Pore formers or metabolic inhibitors in bacteria? *Nat. Rev. Microbiol.* **2005**, 3, 238-250.
14. Paslay, L. C.; Abel, B. A.; Brown, T. D.; Koul, V.; Choudhary, V.; McCormick, C. L.; Morgan, S. E., Antimicrobial Poly(methacrylamide) Derivatives Prepared via Aqueous RAFT Polymerization Exhibit Biocidal Efficiency Dependent upon Cation Structure. *Biomacromolecules* **2012**, 13, 2472-2482.
15. Schmidt, N.; Mishra, A.; Lai, G. H.; Wong, G. C. L., Arginine-rich cell-penetrating peptides. *Febs Letters* **2010**, 584 (9), 1806-1813.
16. Nakase, I.; Takeuchi, T.; Tanaka, G.; Futaki, S., Methodological and cellular aspects that govern the internalization mechanisms of arginine-rich cell-penetrating peptides. *Advanced Drug Delivery Reviews* **2008**, 60 (4-5), 598-607.

17. Treat, N. J.; Smith, D.; Teng, C.; Flores, J. D.; Abel, B. A.; York, A. W.; Huang, F.; McCormick, C. L., Guanidine-Containing Methacrylamide (Co) polymers via a RAFT: Toward a Cell-Penetrating Peptide Mimic. *ACS macro letters* **2011**, *1* (1), 100-104.
18. Convertine, A. J.; Benoit, D. S.; Duvall, C. L.; Hoffman, A. S.; Stayton, P. S., Development of a novel endosomolytic diblock copolymer for siRNA delivery. *Journal of Controlled Release* **2009**, *133* (3), 221-229.
19. Vasilieva, Y. A.; Scales, C. W.; Thomas, D. B.; Ezell, R. G.; Lowe, A. B.; Ayres, N.; McCormick, C. L., Controlled/living polymerization of methacrylamide in aqueous media via the RAFT process. *Journal of Polymer Science Part A: Polymer Chemistry* **2005**, *43* (14), 3141-3152.
20. Gulati, N.; Rastogi, R.; Dinda, A. K.; Saxena, R.; Koul, V., Characterization and cell material interactions of PEGylated PNIPAAm nanoparticles. *Colloids and Surfaces B: Biointerfaces* **2010**, *79* (1), 164-173.
21. Avanti® Mini-Extruder. Avanti Polar Lipids, Inc.
http://www.avantilipids.com/index.php?option=com_content&view=article&id=185&Itemid=193 (accessed March 10, 2014).
22. Stanzl, E. G.; Trantow, B. M.; Vargas, J. R.; Wender, P. A., Fifteen Years of Cell-Penetrating, Guanidinium-Rich Molecular Transporters: Basic Science, Research Tools, and Clinical Applications. *Accounts of Chemical Research* **2013**, *46* (12), 2944-2954.